Supporting Information

High Energy Storage Performance of Random Norbornene Copolymer Containing Oligothiophene as Side-chain for Dielectric Capacitors Applications

Bo Li, [ab] Chenjun Mei [ab], Weili Li, [b] Hui Tong, [ab] Hongkun Tian, *[ab] and Lixiang Wang*[ab]

a. State Key Laboratory of Polymer Science and Technology, Changchun Institute of Applied Chemistry, Chinese Academy of Sciences, Changchun 130022, China. E-mail: hktian@ciac.ac.cn, lixiang@ciac.ac.cn

b. School of Applied Chemistry and Engineering, University of Science and Technology of China, Hefei, 230026, China.

Experimental Procedures

Materials: Exo-3,6-epoxy-1,2,3,6-tetrahydrophthalic anhydride (**1,** 97%), *m*-aminobenzotrifluoride (99%), 2,2,2-trifluoroethylamine (99%), 4-dimethyl-aminopyridine (98%), 2,5-dibromothiophene (98%), 1,4-dibromobutane (98%), tetrakis(triphenylphosphine)palladium (99%), 2-(tributylstannyl)thiophene (97%), *n*-butyllithium (2.5 M) and cyclopentanone (99%) were purchased from Energy Chemical (China).

Characterization: The ^{1}H-NMR spectra were recorded on a Bruker AVANCE III 400 MHz and 500 MHz spectrometer. The number-average molecular weight (M_n) and polydispersity index (PDI) of the polymers synthesized in this work were measured using an Agilent G7129A with THF as the mobile phase. Differential scanning calorimetry (DSC) thermograms of the polymers were obtained by a TA Q2000 DSC instrument under a nitrogen atmosphere at a scanning rate of 5 ^{o}C min^{-1}. Film X-ray diffraction (XRD) measurements were performed on Brucker D8 ADVANCE, with a scanning angle range of 2° to 40°, and equipped with a Cu K_α source (λ = 1.54 Å). Bandgap measurements were performed using PerkinElmer UV/VIS Spectrometer Lambda 35. Scanning Electron Microscopy (SEM) tests were performed on Sigma 300, with film samples cryo-fractured in liquid nitrogen. Dielectric properties were measured with an Agilent LCR instrument (4294A). The dielectric displacement versus electric field (D-E) hysteresis loops were obtained using a PolyK (PK CPE20B) with a modified Sawyer-Tower circuit, where the dielectric films were exposed to a triangular unipolar wave at a frequency of 100 Hz. Dielectric breakdown strength was recorded with a Trek 610C at a voltage rise of 500 V s^{-1}. The experiment was conducted in a silicone oil bath to mitigate surface corona discharge, the breakdown field strengths were measured at 10 electrode points on the polymer film to construct the Weibull distribution plot. Thermally stimulated depolarization currents (TSDC) curves were tested by Keithley 6517B and Huace 450P (Beijing Hauce Testing Instruments Co., Ltd.). Leakage currents were evaluated with a Keithley 6517A electrometer.

Density Functional Theory (DFT) and Molecular Dynamics (MD) Analysis: Dipole moment calculations and molecular frontier orbital energy levels were performed using Gaussian 09. The structures were geometrically optimized using the DFT method at the B3LYP theory level, with the 6–31G(d,p) basis set for molecular orbital energy calculations. Subsequently, the results were visualized using Multiwfn[1-3] and VMD[4]. Amorphous cells were generated, with each cell consisting of 15 molecular chains, polymerized from 30 units. Molecular dynamic simulations were conducted under isothermal (NVT) and isoenergetic equilibration (NVE) conditions, with at least five annealing processes performed on the amorphous cells of all polymers.

Synthesis of TA, TM and TP

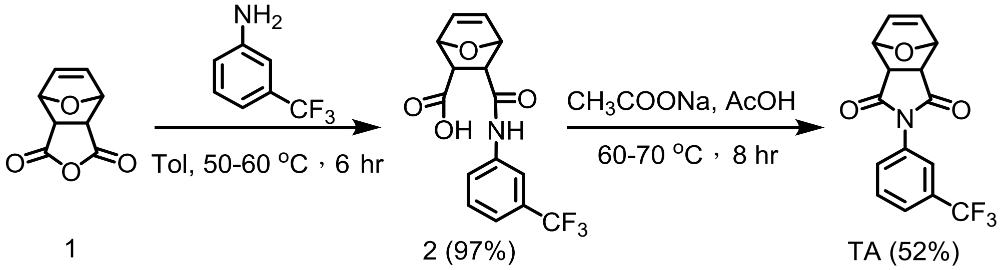

Scheme S1. Schematic of the monomer TA synthesis.

Synthesis of TA: Compound exo-3,6-epoxy-1,2,3,6-tetrahydrophthalic anhydride (**1**, 10 g, 60.19 mmol) and compound *m*-aminobenzotrifluoride (14.55 g, 90.29 mmol) were added to a 500 mL round-bottom flask. The reaction was carried out in 50 mL of toluene at 55 °C for 6 hours. The reaction mixture formed a white emulsion. After filtration and drying, the product **2** was obtained as a white solid (19.23 g) without further purification. Then, compound **2** (12 g, 36.67 mmol) and anhydrous sodium acetate (1.5 g, 18.33 mmol) were added into a 100 mL round-bottom flask and reacted in 35 mL of acetic anhydride solution at 70 °C for 8 hours. The reaction mixture gradually changed from a yellow solution to a brown solution. The mixture was then filtered to remove a white solid, yielding a brown liquid. This liquid was slowly poured into ice-water, resulting in the precipitation of a white product. The solid was collected by suction filtration and dissolved in dichloromethane. The resulting solution was washed with saturated brine to remove residual water, followed by successive stirring with anhydrous sodium sulfate and anhydrous magnesium sulfate for 1 hour each. After filtration, the dichloromethane was removed under rotary evaporation. Recrystallization from ethanol/*n*-hexane gave 5.94 g of product TA, corresponding to a yield of 52%. ^{1}H NMR (500 MHz, DMSO-d$_6$): δ 7.82 (d, *J* = 10 Hz, 1H), 7.76 (t, *J* = 5.0 Hz, 1H), 7.60 (s, 1H), 7.58 (d, *J* = 10.0 Hz, 1H), 6.62 (s, 2H), 5.28 (s, 1H), 3.12 (s, 2H).

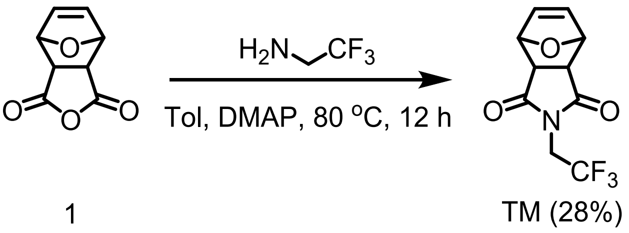

Scheme S2. Schematic of the monomer TM synthesis.

Synthesis of TM: 2,2,2-Trifluoroethylamine (4 g, 40 mmol) dissolved in 20 mL of toluene was added dropwise to a solution of compound **1** (8 g, 48.16 mmol) in 200 mL of toluene. After the addition of 4-dimethylaminopyridine (DMAP, 0.977 g, 8 mmol), the mixture was stirred and heated to 80 °C. After 12 hours, the clear solution turned into a reddish-brown turbidity. The resulting liquid was filtered, concentrated under rotary evaporation, and washed with ethanol to remove yellow impurities, yielding 2.79 g of TM with a yield of 28%. ^{1}H NMR (500 MHz, CDCl$_3$): δ 6.55 (s, 2H), 5.32 (s, 2H), 4.12 (q, *J* = 10.0 Hz, 2H), 2.97 (s, 2H). ^{13}C NMR (125 MHz, CDCl$_3$): δ 174.67, 136.62, 126.25, 124.03, 121.80, 119.58, 81.16, 47.55, 40.11, 39.82, 39.53, 39.24. ^{19}F NMR (470 MHz, CDCl$_3$): δ -70.08, -70.10, -70.12.

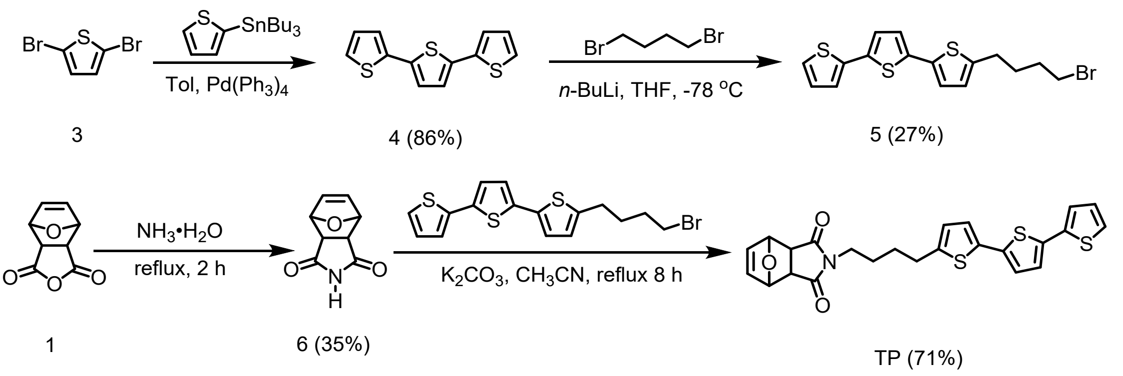

Scheme S3. Schematic of the monomer TP synthesis.

Synthesis of 5: 2,5-Dibromothiophene (**4**, 14.73 g, 60.88 mmol), tetrakis(triphenylphosphine)palladium (3.52 g, 3.046 mmol), and 2-(tributylstannyl)thiophene (50 g, 133.98 mmol) were sequentially added to a 2 L round-bottom flask. The mixture was heated to 110 °C in a toluene/DMF (4:1 400 mL/100 mL) solvent system and reacted overnight. A gradual color change from reddish-brown transparent solution to dark suspension was observed. The reaction was quenched with saturated aqueous KF solution and filtered. The filtrate was extracted with dichloromethane, concentrated under rotary evaporation, and purified by gradient column chromatography. This was achieved by slowly adding pure petroleum ether to a 1:5 (v/v) dichloromethane/petroleum ether mixture. 13.06 g of 2,2':5',2''-terthiophene (**5**)[5] was obtained, corresponding to an 86% yield.

Synthesis of 6: Compound **5** (5.29 g, 21.30 mmol) was dissolved in 110 mL of freshly distilled THF under a nitrogen atmosphere. The solution was cooled to -78 °C in a dry ice/acetone bath, followed by the dropwise addition of 2.5 M *n*-butyllithium in hexanes (10.2 mL, 25.5 mmol). After stirring at low temperature for 1 hour and subsequently at room temperature for 1 hour, the reaction mixture was re-cooled to -78 °C. 1,4-Dibromobutane (5.52 g, 25.56 mmol) was then added, and the reaction was stirred overnight. The system transitioned from a yellow suspension to an orange emulsion. The reaction was quenched with water, filtered, and the filtrate was extracted with ethyl acetate. The combined organic layers were dried over anhydrous Na_2SO_4, filtered, and concentrated. Purification by gradient column chromatography (eluent: petroleum ether and petroleum ether/dichloromethane 12:1 v/v) afforded 2.19 g of the brominated intermediate **6,** corresponding to a yield of 27%. ^{1}H NMR (500 MHz, $CDCl_3$): δ 7.20 (dd, *J* = 1.2, 5.0 Hz, 1H), 7.15 (dd, *J* = 1.2, 3.6 Hz, 1H), 7.05 (d, *J* = 3.8 Hz, 1H), 7.01 (dd, *J* = 3.6, 5.1 Hz, 1H), 7.00 (d, *J* = 3.7 Hz, 1H), 6.98 (d, *J* = 3.5 Hz, 1H), 6.71 (d, *J* = 3.5 Hz, 1H), 3.44 (t, *J* = 6.5 Hz, 2H), 2.84 (t, *J* = 6.5 Hz, 2H), 1.94 (m, 2H), 1.85 (m, 2H).

Synthesis of 7: Compound **1** (30 g, 180.58 mmol) was added to 100 mL of aqueous ammonia and 20 mL of deionized water, and the reaction was carried out at 110 °C, resulting in a yellow transparent solution. After 4 hours, the mixture was allowed to cool and crystals were obtained by precipitation. The product was filtered and washed with n-hexane to yield a white crystalline product **7** (10.44 g, 35%). ^{1}H NMR (500 MHz, DMSO-d_6): δ 10.11 (s, 1H), 6.53 (s, 2H), 5.11 (s, 2H), 2.85 (s, 2H).

Synthesis of TP: Compound **7** (1.34 g, 8.12 mmol), Compound **6** (3.74 g, 9.741 mmol), and K_2CO_3 pellets (2.24 g, 16.23 mmol) were combined in 127 mL of acetonitrile. The mixture was heated under reflux at 91 °C for 8 hours, resulting in a deep red solution. After cooling, insoluble solids were removed by filtration. The filtrate was concentrated and purified by column chromatography using a gradient eluent of dichloromethane, gradually adding ethyl acetate. This afforded 2.71 g of product TP (71% yield). ^{1}H NMR (400 MHz, $CDCl_3$): δ 7.20 (dd, *J* = 1.2, 5.0 Hz, 1H), 7.15 (dd, *J* = 1.2, 3.6 Hz, 1H), 7.05 (d, *J* = 3.8 Hz, 1H), 7.00 (dd, *J* = 3.6, 5.1 Hz, 1H), 6.98 (d, *J* = 3.8 Hz, 1H), 6.96 (d, *J* = 3.6 Hz, 1H), 6.67 (d, *J* = 3.6 Hz, 1H), 6.49 (s, 2H), 5.26 (s, 2H), 3.51 (t, *J* = 5.7 Hz, 2H), 2.82 (s, 2H), 2.80 (t, *J* = 7.0 Hz, 2H), 1.65 (m, 4H). ^{13}C NMR (125 MHz, $CDCl_3$): δ 176.28, 144.43, 137.27, 136.67, 136.54, 135.58, 134.73, 127.85, 125.19, 124.30, 124.26, 123.62, 123.52, 123.44, 80.92, 47.40, 38.47, 29.50, 28.46, 26.88.

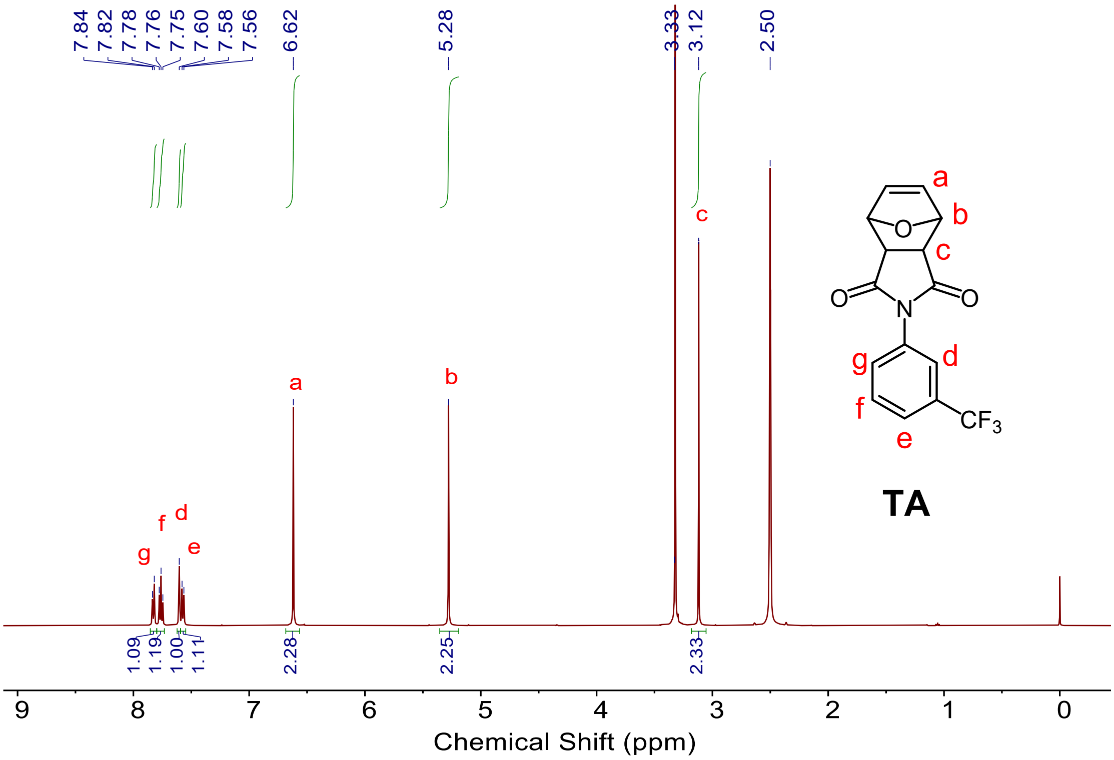

Figure S1. ^{1}H-NMR (500 MHz, DMSO-d_6) spectrum of monomer TA.

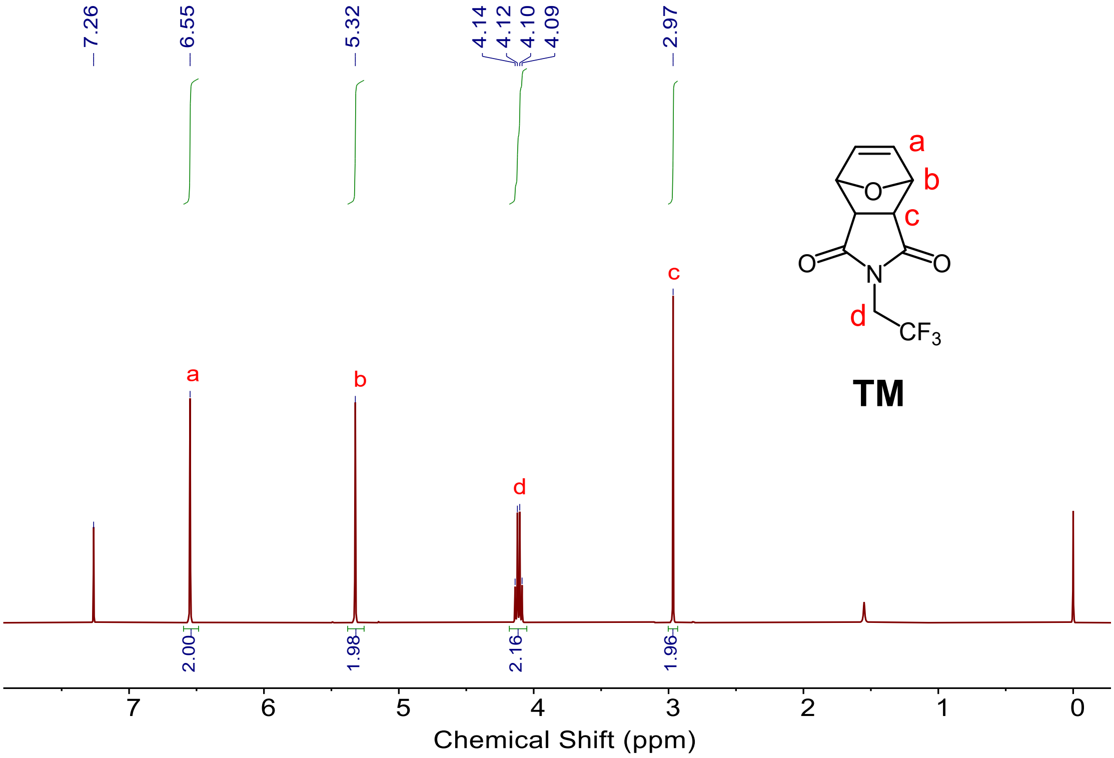

Figure S2. ^{1}H-NMR (500 MHz, $CDCl_3$) spectrum of monomer TM.

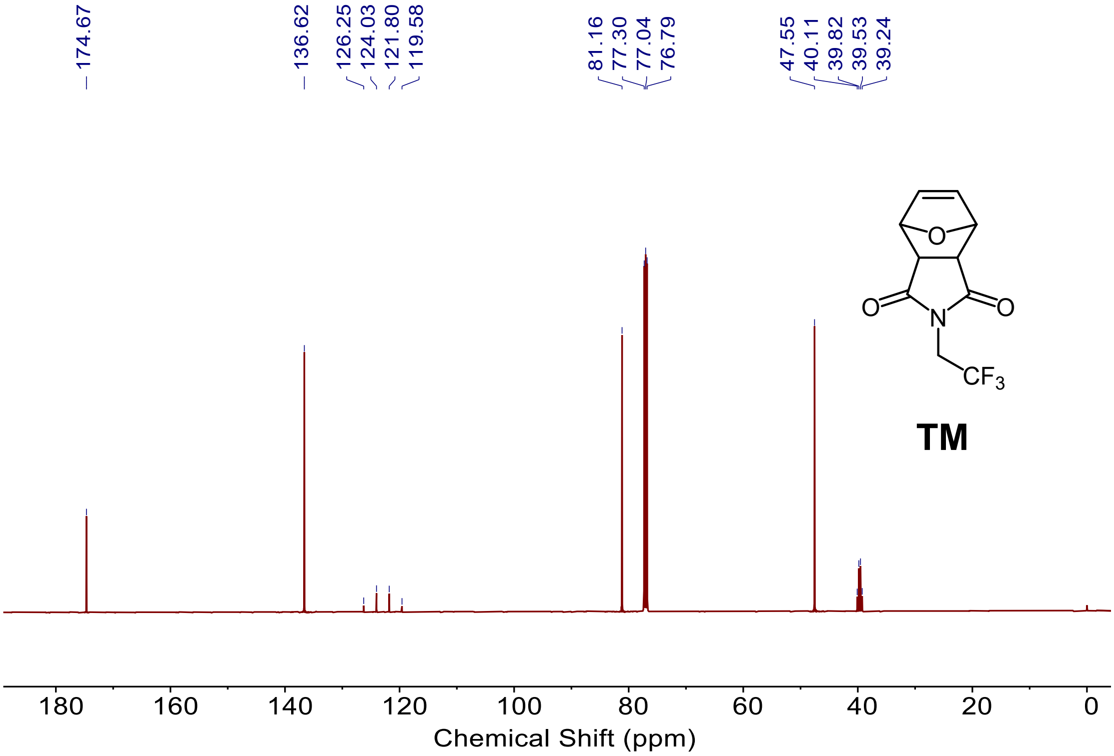

Figure S3. ^{13}C-NMR (125 MHz, $CDCl_3$) spectrum of monomer TM.

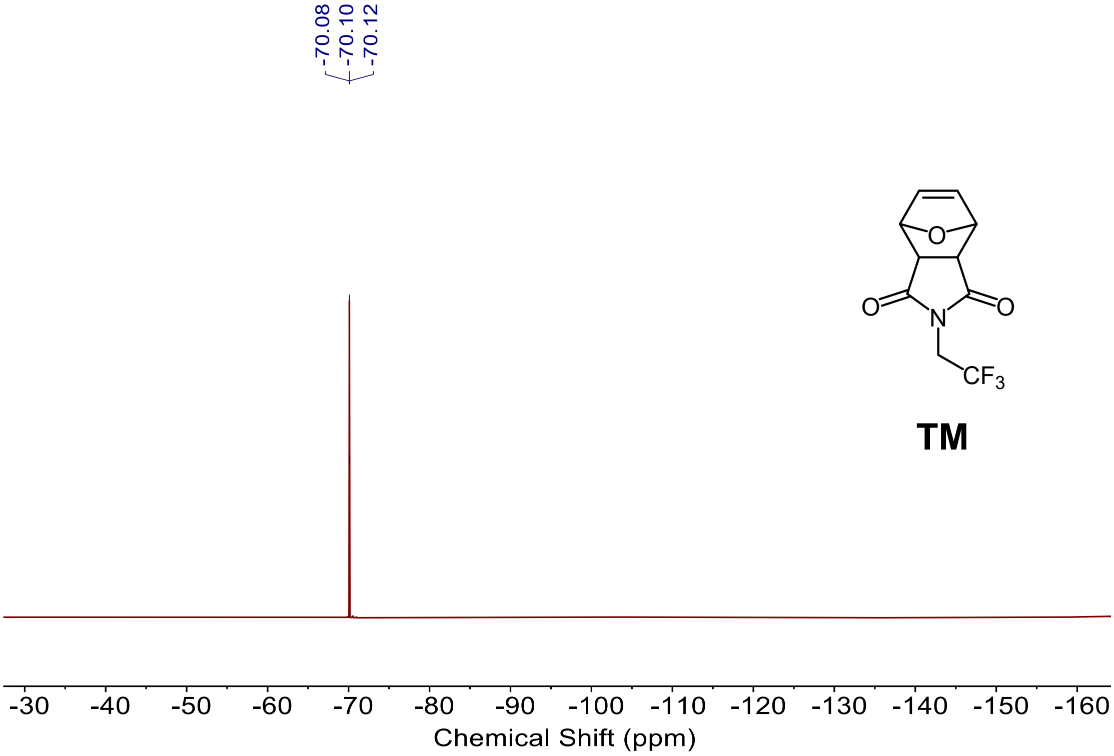

Figure S4. ^{19}F-NMR (470 MHz, $CDCl_3$) spectrum of monomer TM.

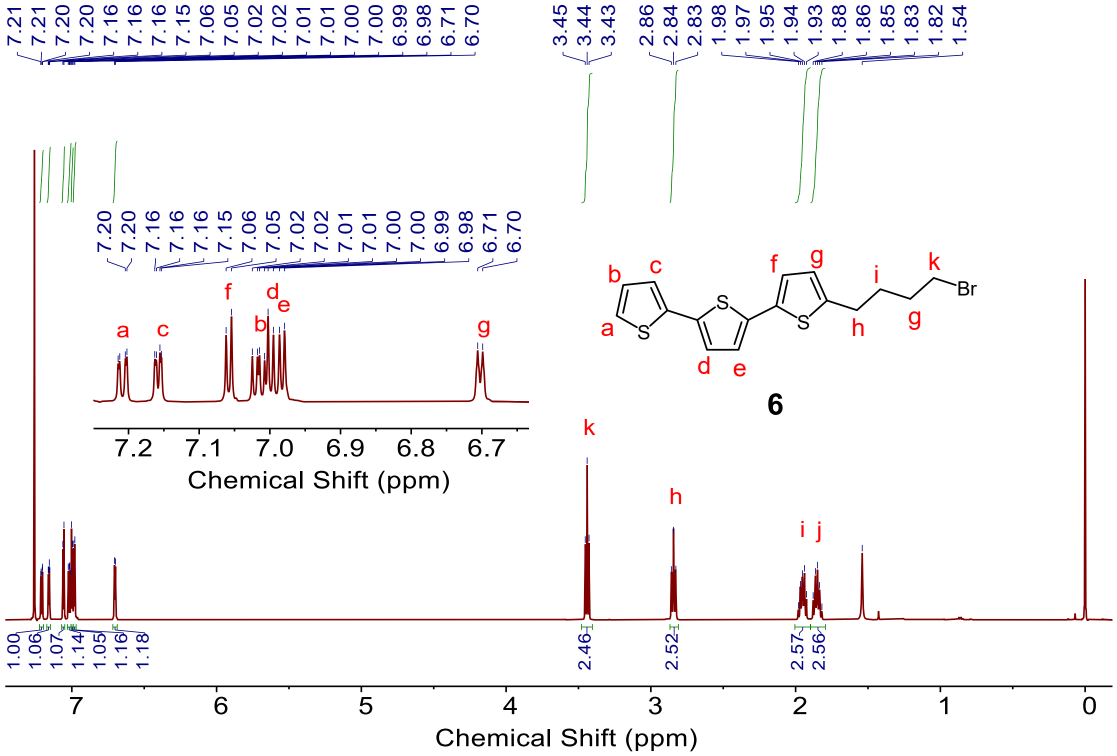

Figure S5. ^{1}H-NMR (500 MHz, $CDCl_3$) spectrum of compound **6**.

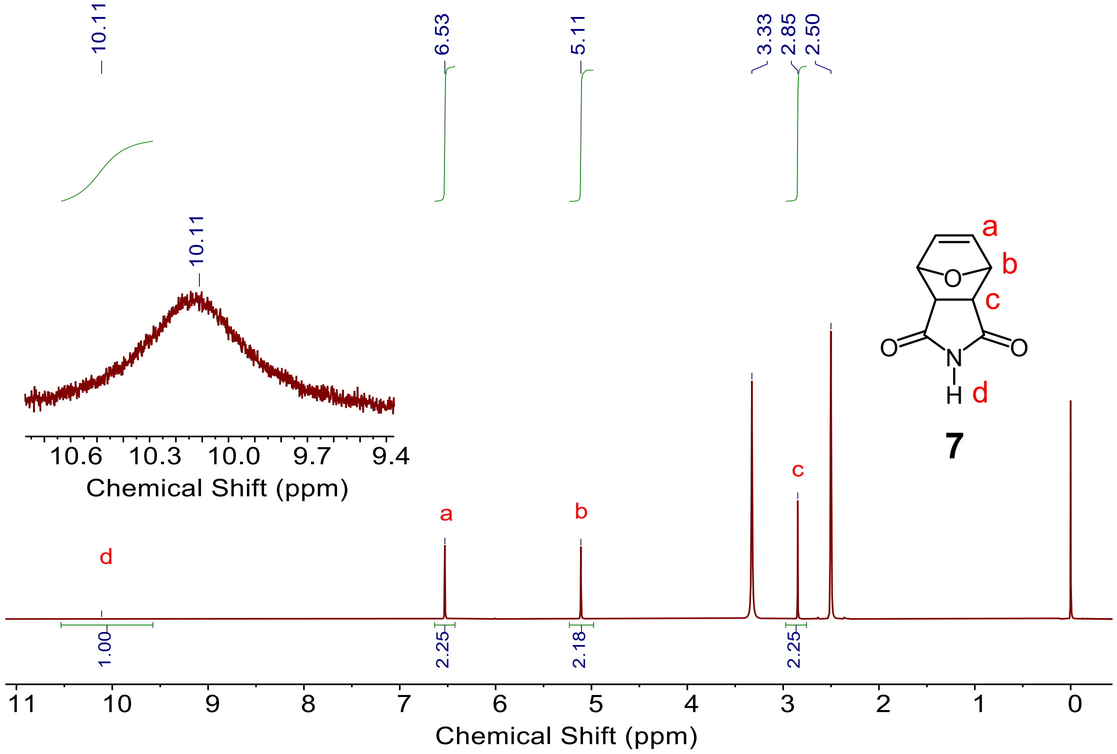

Figure S6. ^{1}H-NMR (500 MHz, DMSO-d_6) spectrum of compound **7**.

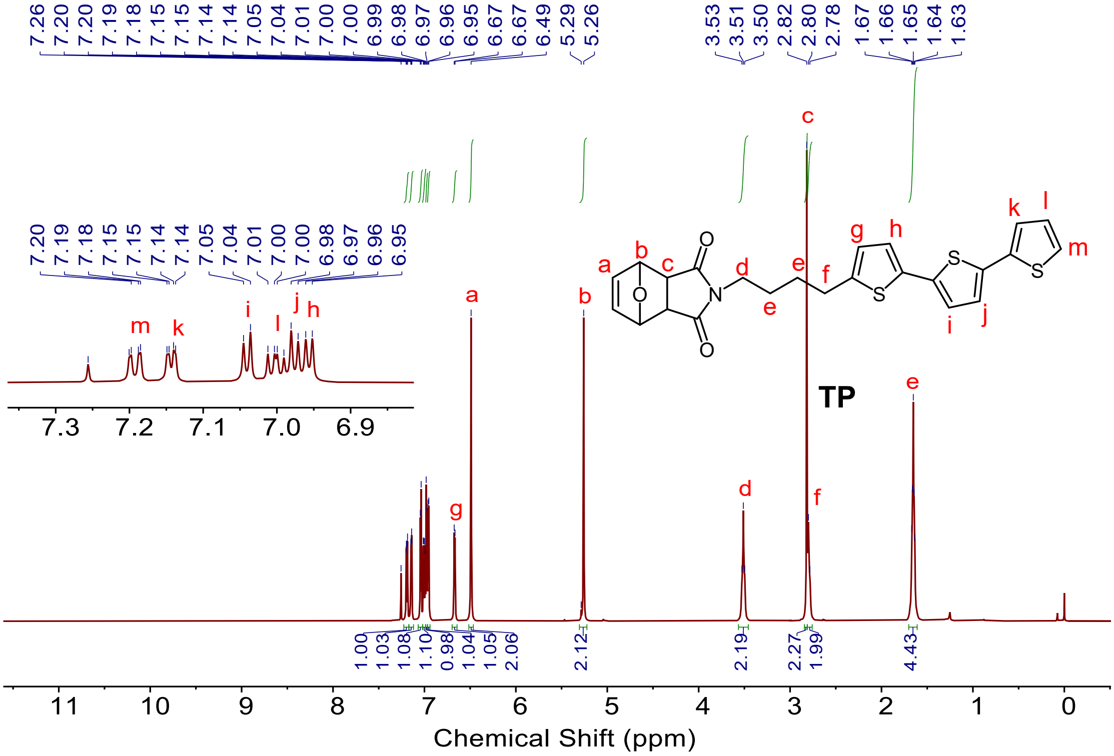

Figure S7. ^{1}H-NMR (400 MHz, $CDCl_3$) spectrum of monomer TP.

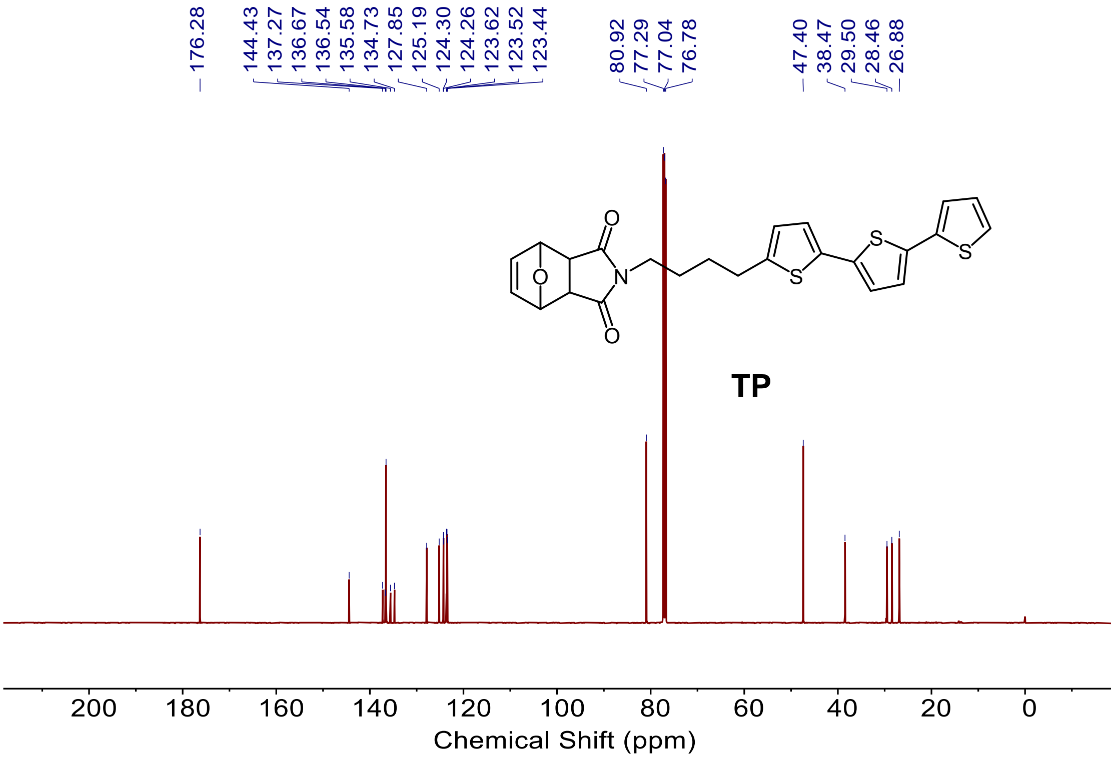

Figure S8. ^{13}C-NMR (125 MHz, $CDCl_3$) spectrum of monomer TP.

Polymerization of TA, TM and TP

Polymerization of PTA-TP: TA (2.0 g, 6.467 mmol) and TP (81.64 mg, 0.175 mmol) were dissolved in 16 mL of anhydrous dichloromethane, while the Grubbs III catalyst (23.43 mg, 0.0265 mmol) was dissolved in 4 mL of anhydrous dichloromethane. The solution was then transferred to the reaction system. The reaction was carried out at room temperature for 3 hours, after which 1 mL of vinyl ethyl ether was added to terminate the reaction. The polymer was precipitated in HPLC-grade methanol to yield polymer PTA-TP-1.

The synthesis of PTA, PTA-TP-3, PTA-TP-4, and PTA-TP-7 followed the same procedure, with the amounts of TP being 0 mg, 136.1 mg (0.291 mmol), 181.45 mg (0.388 mmol), and 272.17 mg (0.582 mmol), respectively.

Polymerization of PTM-TP: TM (1.0 g, 4.046 mmol) and TP (85.14 mg, 0.182 mmol) were dissolved in 14 mL of anhydrous THF, while the Grubbs III catalyst (14.66 mg, 0.0166 mmol) was dissolved in 2 mL of anhydrous THF. The solution was then transferred to the reaction system. The reaction was carried out at room temperature for 3 hours, after which 0.5 mL of vinyl ethyl ether was added to terminate the reaction. The polymer was precipitated in HPLC-grade methanol to yield polymer PTM-TP-4.

The synthesis of PTM, PTM-TP-3, and PTM-TP-5 followed the same procedure, with TP amounts of 0 mg, 85.13 mg (0.182 mmol), and 113.51 mg (0.243 mmol), respectively.

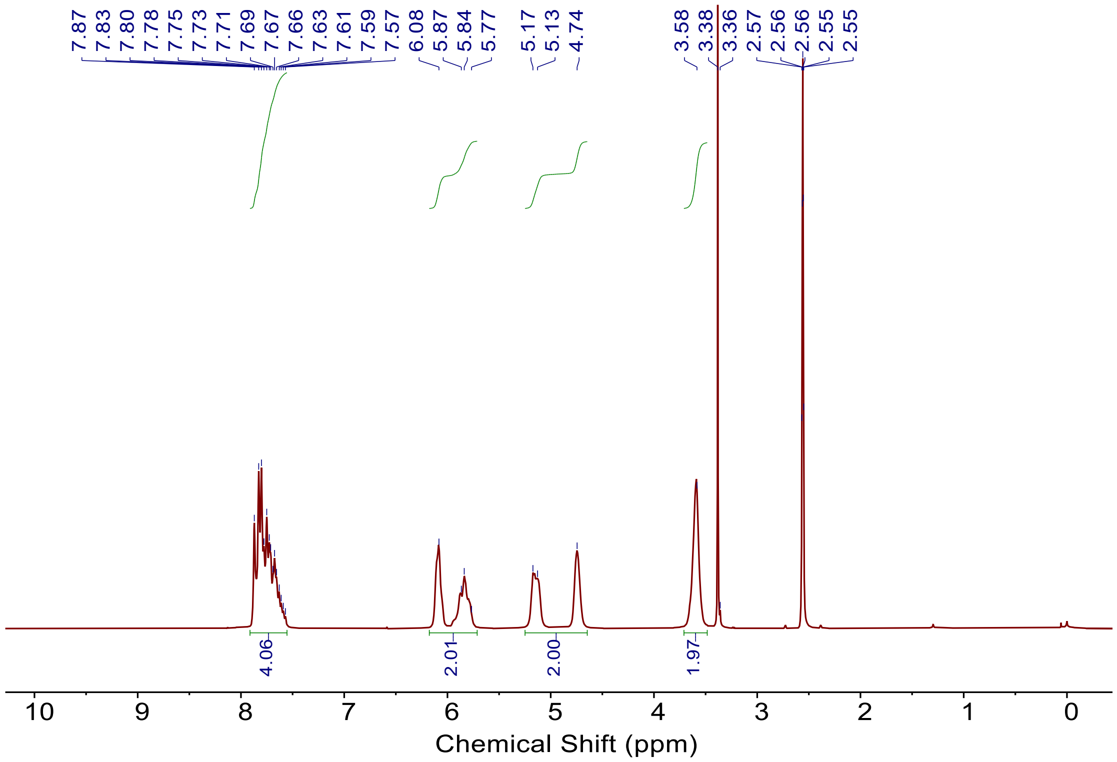

Figure S9. ^{1}H-NMR (500 MHz, DMSO-d_6) spectrum of PTA.

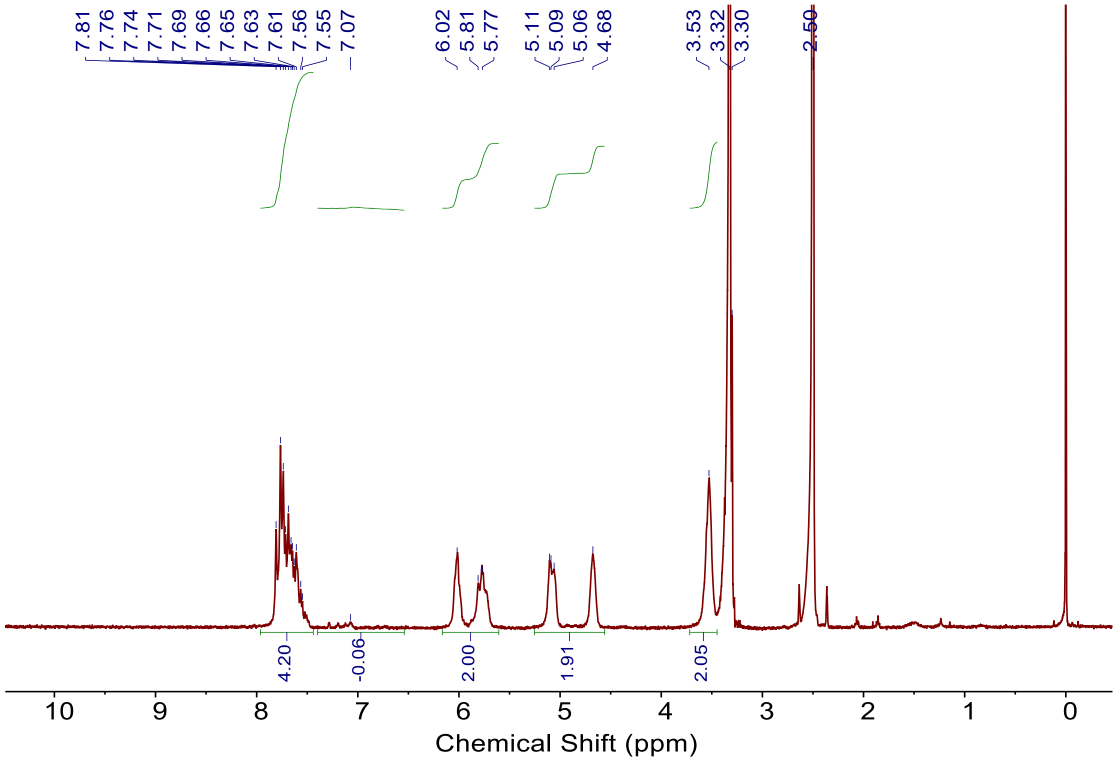

Figure S10. ^{1}H-NMR (500 MHz, DMSO-d_6) spectrum of PTA-TP-1.

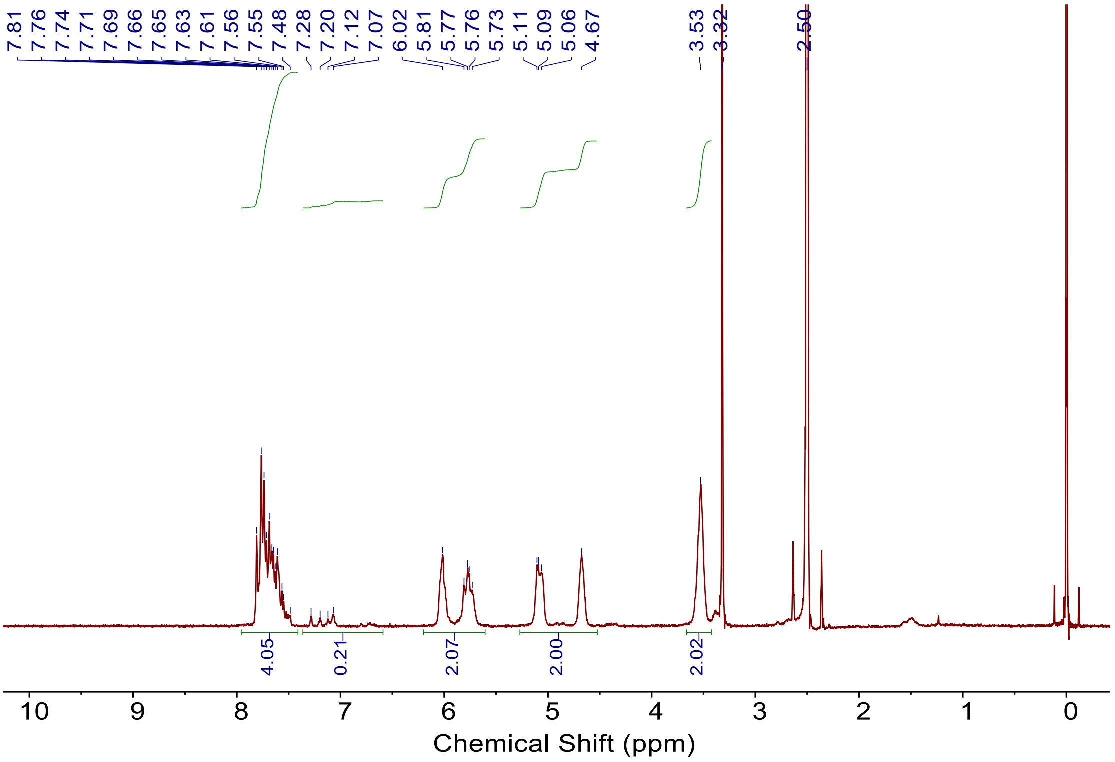

Figure S11. ^{1}H-NMR (500 MHz, DMSO-d$_6$) spectrum of PTA-TP-3.

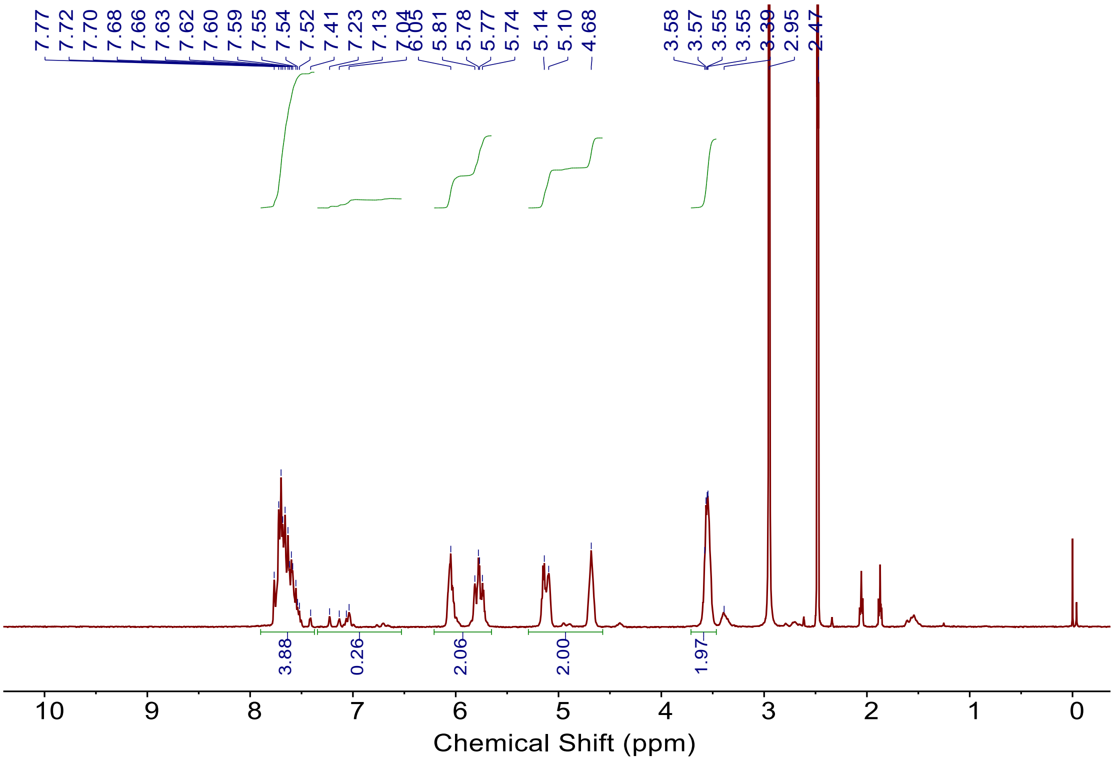

Figure S12. ^{1}H-NMR (500 MHz, DMSO-d$_6$) spectrum of PTA-TP-4.

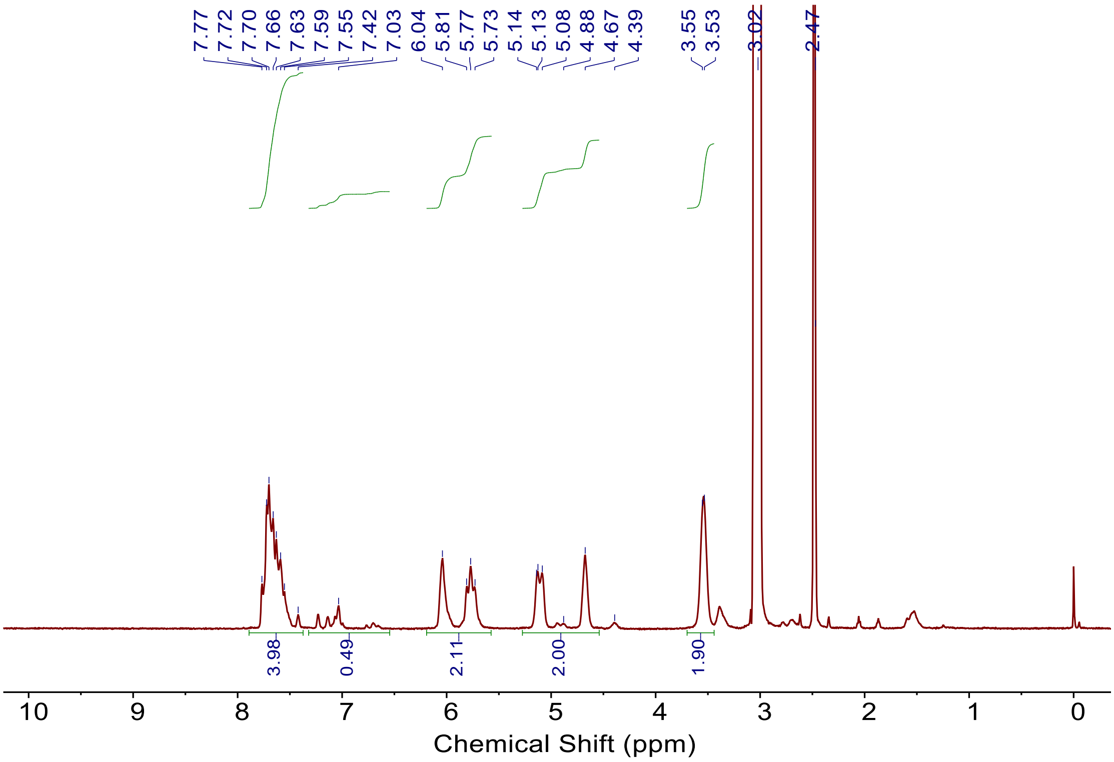

Figure S13. ^{1}H-NMR (500 MHz, DMSO-d_6) spectrum of PTA-TP-7.

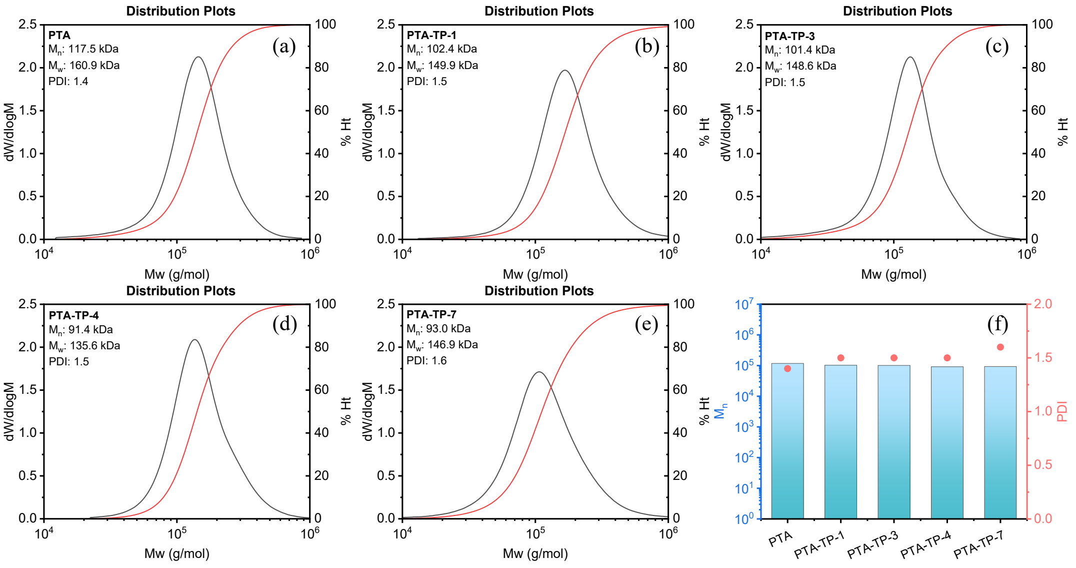

Figure S14. M_n and PDI values of PTA-TP polymers characterized by GPC with tetrahydrofuran (THF) as the mobile phase.

Preparation of the film: The synthesized polymers (PTA and PTA-TP) were dissolved in cyclopentanone and drop-cast onto a glass substrate to form films. For D-E loop, Weibull analysis, leakage current, TSDC, and cycling stability tests, the film thickness is approximately 10 µm. For temperature-dependent dielectric and frequency-dependent dielectric spectrum, the film thickness is approximately 50 µm. The film thickness was measured with a micrometer. Considering the coffee-ring effect during drop-casting, a polymer solution of 80 mg mL^{-1} was typically prepared, and 1 mL of this solution was drop-cast onto a 6 × 6 cm glass substrate to obtain a film thickness of 10 µm. To obtain a film thickness of 50 µm, a polymer solution of 225 mg mL^{-1} was prepared, and 0.8 mL of this solution was drop-cast onto a 4 × 4 cm glass substrate. The films were initially dried at room temperature for 12 hours to remove most of the solvent, followed by a gradient heating treatment under vacuum: 1 hour at 70 ^{o}C, 3 hours at 100 ^{o}C, 1 hour at 130 ^{o}C, and 4 hours at 150 ^{o}C. After the gradient heating treatment, the system was naturally cooled to room temperature. The glass substrate with the film was immersed in deionized water to allow the poly(norbornene-imide) film to peel off from the substrate. The resulting films were then used for subsequent characterizations.

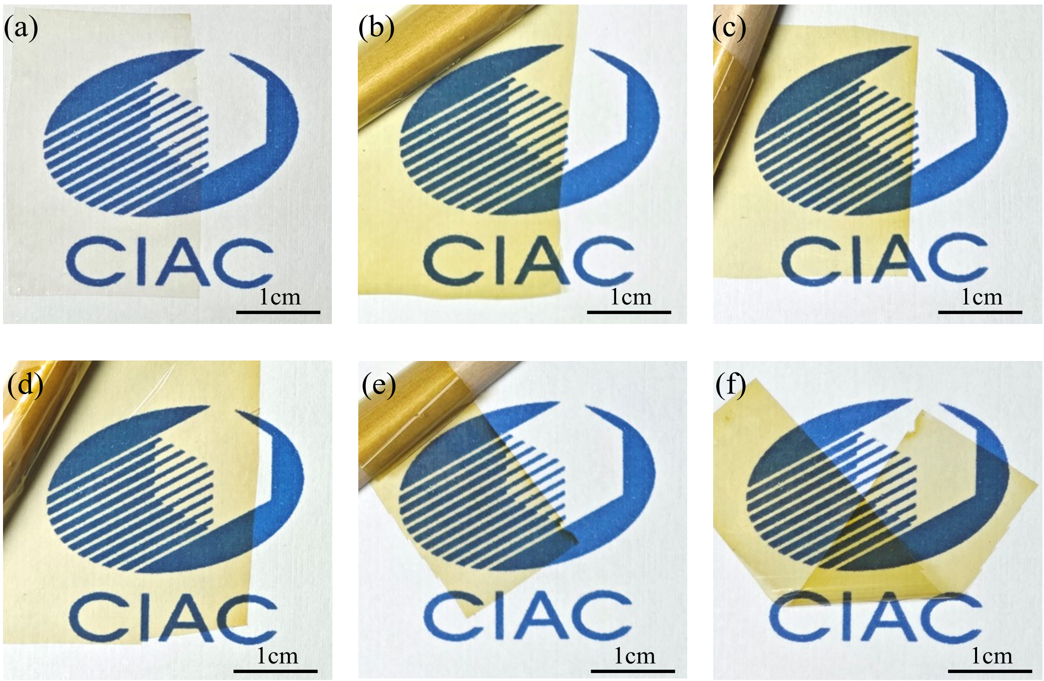

Figure S15. (a), (b), (c), (d) and (e) Digital photographs of PTA, PTA-TP-1, PTA-TP-3, PTA-TP-4 and PTA-TP-7 films (~10 µm); (f) Photograph demonstrating the good flexibility of a PTA-TP film (~10 µm).

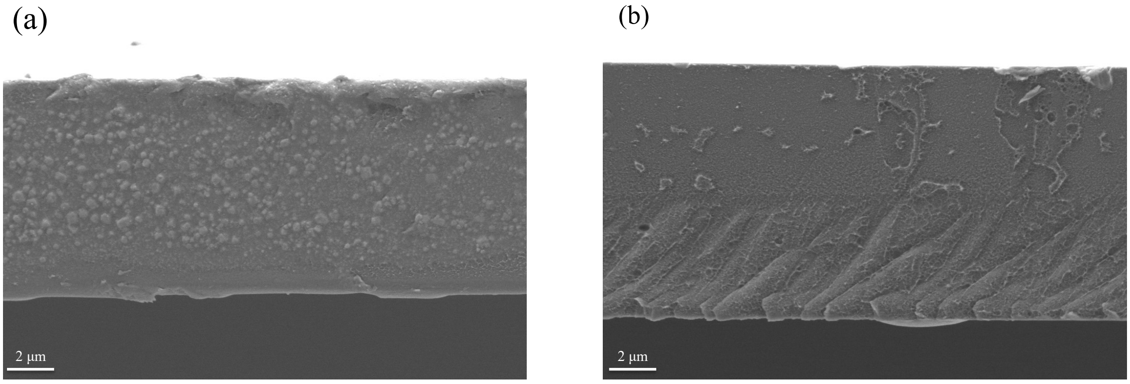

Figure S16. (a) Cross-section SEM image of PTA film; (b) Cross-section SEM image of PTA-TP-3 film.

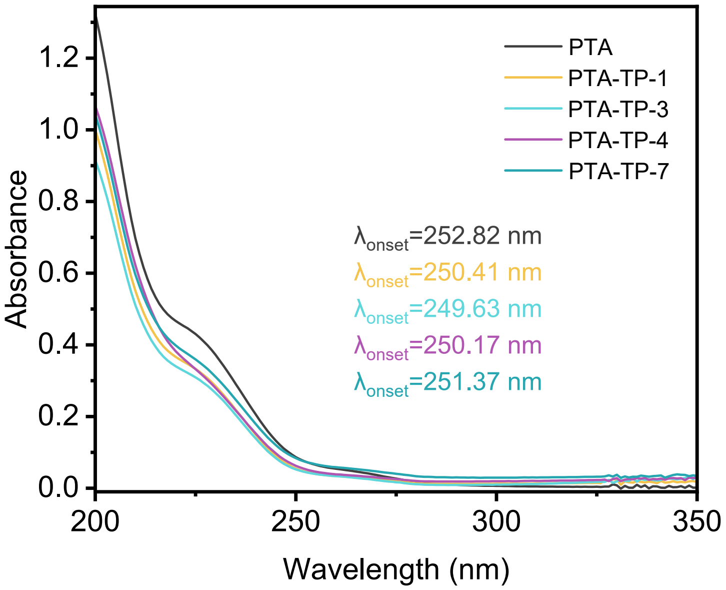

Figure S17. UV-Vis spectra of polymer PTA and copolymers PTA-TP.

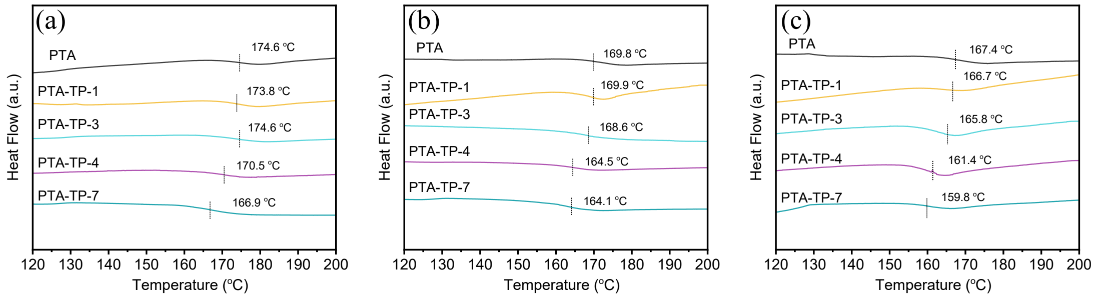

Figure S18. DSC curves of PTA and PTA-TP during the second heating scan from three parallel measurements.

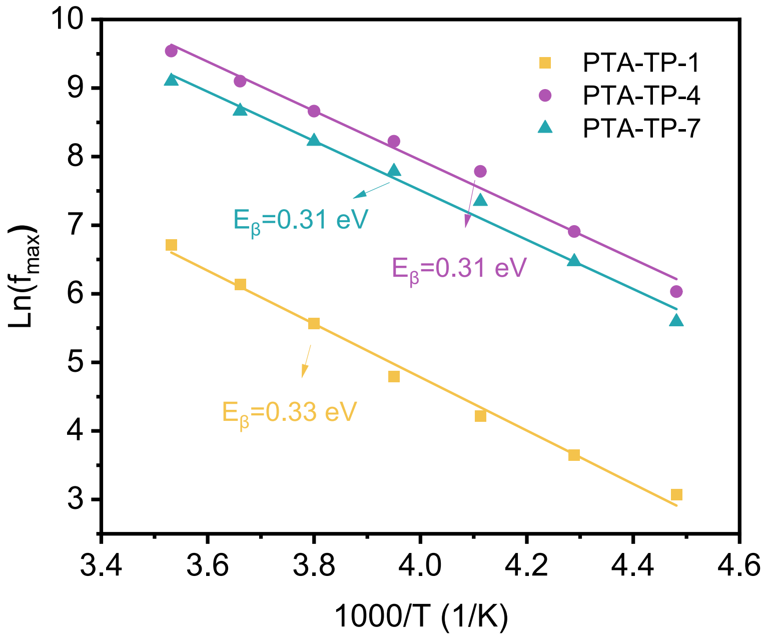

Figure S19. Activation energies for the β transition of PTA-TP-1, PTA-TP-4 and PTA-TP-7.

Table S1. Comparation of PTA and PTA-TP in the dielectric properties.

	Dielectric constant (RT@100 Hz)	Dissipation factor (RT@100 Hz)	Dielectric breakdown strength (MV m^{-1}) (@150 °C)	Maximum discharged energy density (J cm^{-3}) and efficiency (@150 °C)	Discharged energy density (J cm^{-3}) and efficiency (700 MV m^{-1} @150 °C)
PTA	3.35	1.7%	700	7.17 (700 MV m^{-1}); 79%	7.17, 79%
PTA-TP-1	3.53	1.5%	700	8.00 (700 MV m^{-1}); 86%	8.00, 86%
PTA-TP-3	3.59	1.5%	750	9.75 (750 MV m^{-1}); 89%	8.50, 91%
PTA-TP-4	3.73	1.3%	750	9.11 (750 MV m^{-1}); 78%	8.20, 83%
PTA-TP-7	3.93	1.3%	550	5.63 (550 MV m^{-1}); 79%	none

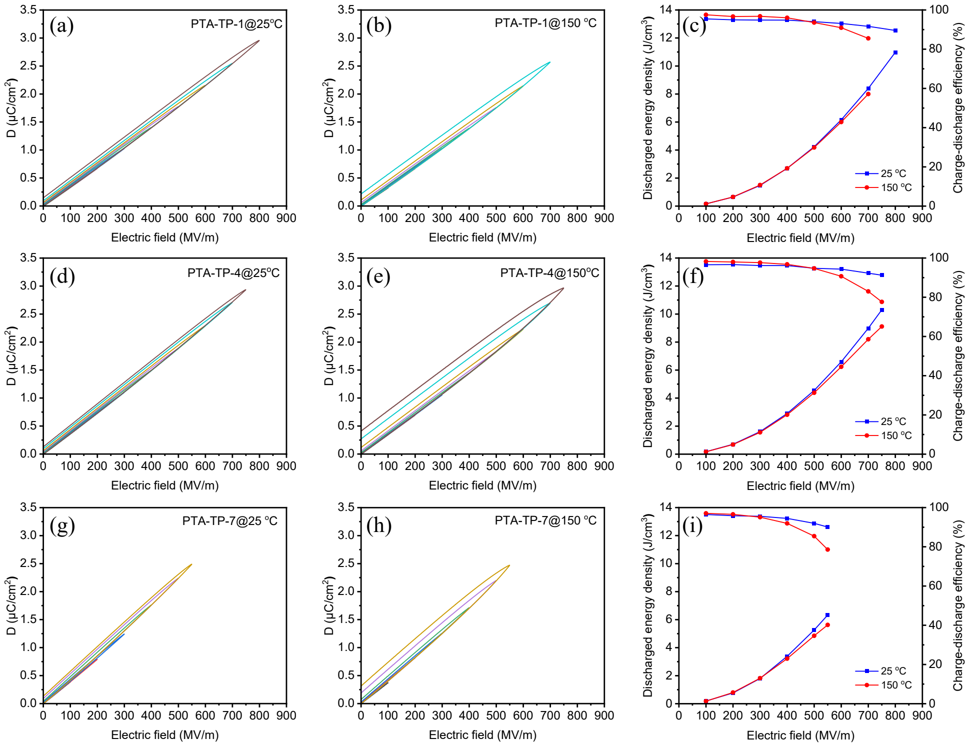

Figure S20. (a), (b), (d), (e), (g) and (h) D–E loops of PTA-TP-1, PTA-TP-4 and PTA-TP-7 at 25 °C and 150 °C; (c), (f) and (i) discharged energy density and efficiency of PTA-TP-1, PTA-TP-4 and PTA-TP-7 at 25 °C and 150 °C.

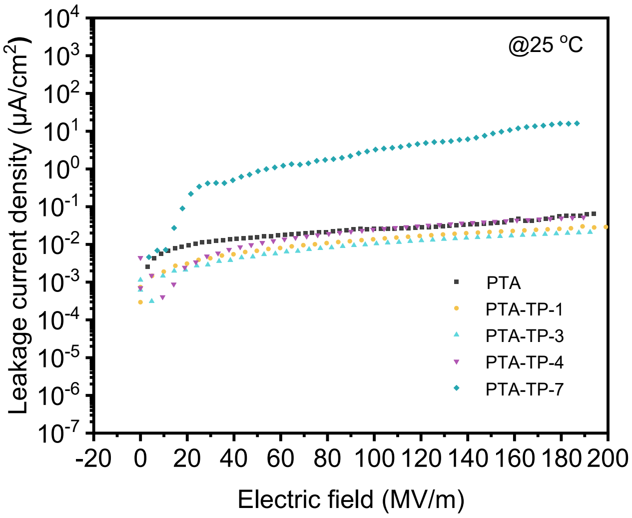

Figure S21. Leakage current as a function of electric field for all polymers at 25 °C

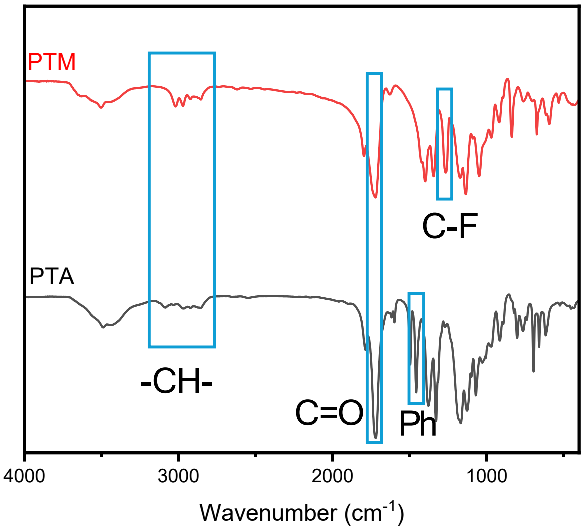

Figure S22. The FT-IR spectra of PTA and PTM.

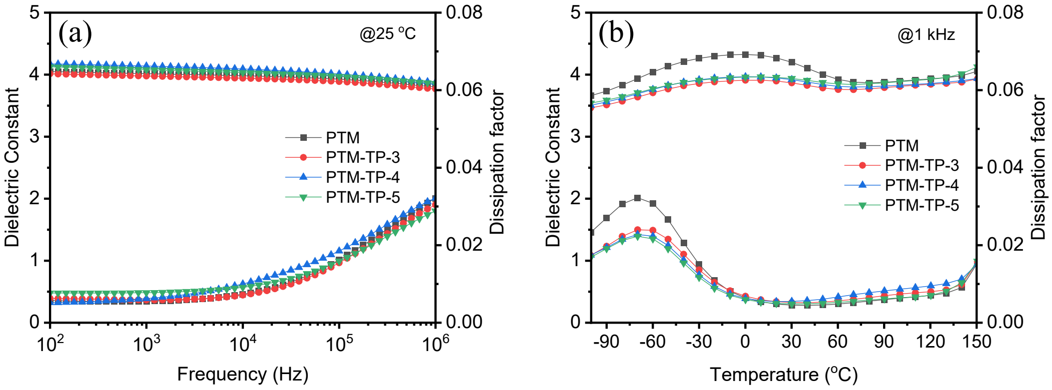

Figure S23. (a) Real dielectric constant and dissipation factor of the fabricated PTM and PTM-TP polymers as a function of frequency at room temperature; (b) real dielectric constant and dissipation factor of the fabricated PTM and PTM-TP polymers as a function of temperature at 1 kHz.

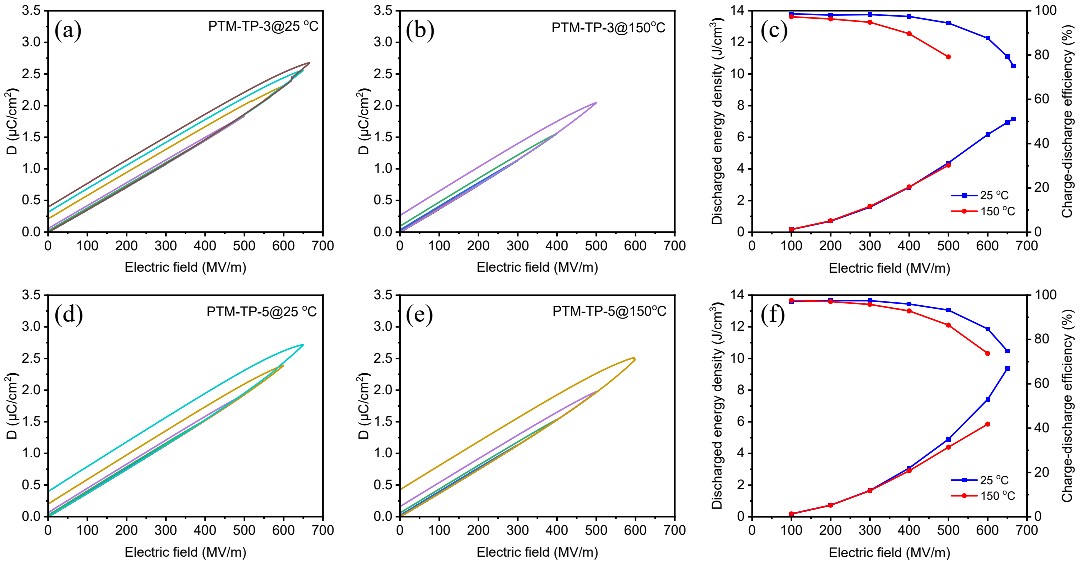

Figure S24. (a), (b), (d) and (e) D–E loops of PTM-TP-3 and PTM-TP-5 at 25 °C and 150 °C; (c) and (f) discharged energy density and discharging efficiency of PTM-TP-3 and PTM-TP-5 at 25 °C and 150 °C.

Table S2. Comparation of PTM and PTM-TP in the dielectric properties.

	Dielectric constant (RT@1 kHz)	Dissipation factor (RT@1 kHz)	Dielectric breakdown strength (MV m^{-1}) (@150 ^{o}C)	Maximum discharged energy density (J cm^{-3}) and efficiency (@150 ^{o}C)
PTM	3.93	1.6%	400	2.42 (400 MV m^{-1}); 69.4%
PTM-TP-3	3.89	1.5%	500	4.24 (500 MV m^{-1}); 79.1%
PTM-TP-4	3.9	1.6%	600	5.94 (600 MV m^{-1}); 73.7%
PTM-TP-5	4.01	1.9%	600	5.86 (600 MV m^{-1}); 73.7%

References

1 T. Lu, *J. Chem. Phys.*, 2024, **161**, 082503.

2 T. Lu and F. Chen, *J. Theor. Comput. Chem.*, 2012, **11**, 163-183.

3 T. Lu and F. Chen, *J. Comput. Chem.*, 2012, **33**, 580-592.

4 W. Humphrey, A. Dalke and K. Schulten, *J. Mol. Graph.*, 1996, **14**, 33-38.

5 T. A. Ranathunge, D. Karunathilaka, D. T. Ngo, N. H. Attanayake, P. Brodgon, J. H. Delcamp, R. M. G. Rajapakse and D. L. Watkins, *Macromol. Chem. Phys.*, 2019, **220**, 1900289.